doi: 10.12029/gc20210113

孔会磊, 栗亚芝, 李金超, 贾群子, 国显正, 王宇, 姚学钢. 2021. 东昆仑希望沟橄榄辉长岩的岩石成因:地球化学、锆石U-Pb年龄与Hf同位素制约[J]. 中国地质, 48(1): 173-188.

Kong Huilei, Li Yazhi, Li Jinchao, Jia Qunzi, Guo Xianzheng, Wang Yu, Yao Xuegang. 2021. Petrogenesis of Xiwanggou olivine gabbro in East Kunlun Mountains: Constraints from geochemistry, zircon U-Pb dating and Hf isotopes[J]. Geology in China, 48(1): 173-188(in Chinese with English abstract).

东昆仑希望沟橄榄辉长岩的岩石成因:地球化学、锆石U-Pb年龄与Hf同位素制约

孔会磊[1,2],栗亚芝[2],李金超[2],贾群子[2],国显正[2,3],王宇[2],姚学钢[2,3]

(1.中国地质科学院,北京 1000372;中国地质调查局西安地质调查中心自然资源部岩浆作用成矿与找矿重点实验室,陕西 西安 710054;3.中国地质大学(武汉)地质调查研究院,湖北 武汉 430074)

提要:东昆仑古特提斯域镁铁-超镁铁质岩石的研究极为薄弱,文章报道了青海东昆仑东段希望沟橄榄辉长岩的岩相学、锆石U-Pb年代学、岩石地球化学及锆石Hf同位素资料,以确定该岩体的形成时代、岩石成因及构造环境,为东昆仑晚古生代—早中生代构造岩浆演化提供新的约束。岩石地球化学研究表明,希望沟橄榄辉长岩具有低SiO_2(40.91%~42.14%)、低TiO_2(0.29%~0.39%)、高MgO(28.18%~30.66%)、贫碱(K_2O+Na_2O=1.09%~1.36%)的特征,属亚碱性系列岩石,m/f比值介于5.03~5.39,属于铁质超基性岩类。岩石微量元素总体上富集大离子亲石元素(Rb、Th、U、K)和Pb,相对亏损高场强元素(Nb、P、Ti),ΣREE为28.17×10^{-6}~30.95×10^{-6},$(La/Yb)_N$为3.77~4.98,显示轻稀土富集的特征,δEu=0.80~0.95,具有弱的Eu负异常。利用LA-ICP-MS锆石U-Pb定年技术,获得橄榄辉长岩加权平均年龄为(264.9±1.2)Ma(n=26,MSWD =0.71),属中二叠世。锆石$^{176}Hf/^{177}Hf$比值为0.282709~0.283152,对应的$\varepsilon_{Hf}(t)$=3.7~19.3,锆石单阶段Hf模式年龄T_{DM}为135~753 Ma,平均为414 Ma,大于锆石U-Pb年龄。研究认为,橄榄辉长岩的岩浆源区主要为亏损地幔,可能有早期流体交代的岩石圈地幔组分的加入,并经历了地壳物质的混染。结合东昆仑区域构造演化,认为希望沟橄榄辉长岩是阿尼玛卿古特提斯洋俯冲阶段的产物,说明古特提斯洋在中二叠世已北向俯冲。

关 键 词: 东昆仑;希望沟橄榄辉长岩;LA-ICP-MS锆石U-Pb测年;地球化学; Hf同位素;地质调查工程

中国分类号:P597;P588.12+.4 **文献标志码**:A **文章编号**:1000-3657(2021)01-0173-16

Petrogenesis of Xiwanggou olivine gabbro in East Kunlun Mountains: Constraints from geochemistry, zircon U-Pb dating and Hf isotopes

KONG Huilei[1,2], LI Yazhi[2], LI Jinchao[2], JIA Qunzi[2], GUO Xianzheng[2,3], WANG Yu[2], YAO Xuegang[2,3]

(1.*Chinese Academy of Geological Sciences, Beijing* 100037,*China*;2.*Key Laboratory for the Study of Focused Magmatism and Giant Ore Deposits, MNR, Xi'an Center of Geological Survey, CGS, Xi'an* 710054*, Shaanxi, China;* 3. *Institute of Geological Survey, China University of Geosciences, Wuhan* 430074*, Hubei, China*)

收稿日期:2018-03-13;**改回日期**:2019-05-18

基金项目:中国地质调查局地质调查项目(DD20190143,DD20160013)、国家重点研发计划课题(2019YFC0605201)和第二次青藏高原综合科学考察研究专题(2019QZKK0807-02)联合资助。

作者简介:孔会磊,男,1985年生,博士生,高级工程师,主要从事区域成矿及成矿规律研究;E-mail: konghuilei2008@126.com。

通讯作者:栗亚芝,女,1979年生,硕士,高级工程师,主要从事区域成矿及成矿规律研究;E-mail: liyazhi2005@163.com。

Abstract: The mafic−ultramafic rocks in Paleo−Tethys domain of East Kunlun Mountains are not well documented. In this paper, the authors present petrographical, geochronological, lithogeochemical and Hf isotopic data for the Xiwanggou olivine gabbro located in the eastern section of East Kunlun Mountains, Qinghai Province, with the purpose of constraining its formation age, petrogenesis and tectonic setting and providing new constraints for the Late Paleozoic−Early Mesozoic tectono−magmatic evolution in East Kunlun Mountains. Lithogeochemical studies show that the olivine gabbro, which is of sub−alkaline series, is characterized by low SiO_2 (40.91%−42.14%), low TiO_2 (0.29%−0.39%) and alkali content (K_2O+Na_2O=1.09%−1.36%) but high MgO content (28.18%−30.66%). The m/f ratios range from 5.03 to 5.39, falling into the field of ferrous−ultrabasic rocks. This suite of rocks are enriched in LILE (such as Rb, Th, U and K) and Pb, and relatively depleted in HFSE (such as Nb, P and Ti). The rocks have low REE content, with LREE−rich pattern and slightly negative Eu anomaly (ΣREE=28.17×10^{-6}−30.95×10^{-6}, $(La/Yb)_N$=3.77−4.98, δEu=0.80−0.95). LA−ICP−MS zircon U−Pb dating indicates that the weighted mean age of olivine gabbro is (264.9±1.2)Ma(n=26, MSWD=0.71), suggesting Middle Permian. Zircon $^{176}Hf/^{177}Hf$ values are in the range of 0.282709−0.283152 with corresponding $\varepsilon_{Hf}(t)$ values of 3.7−19.3. and Lu−Hf single−stage modal ages (T_{DM}) vary from 135 to 753 Ma with mean age being 414Ma, older than U−Pb age. The authors hold that the parental magma of olivine gabbro was likely derived from the depleted mantle, with the probable addition of fluid−modified lithospheric mantle components, and was contaminated by crustal material. Combined with evolutionary characteristics of regional structures in East Kunlun Mountains, the authors consider that Xiwanggou olivine gabbro was formed during the subduction of Anyemaqen−Paleo−Tethys Ocean, and the northward subduction of Anyemaqen−Paleo−Tethys Ocean started at least in Middle Permian.

Key words: East Kunlun Mountains; Xiwanggou olivine gabbro; LA−ICP−MS zircon U−Pb dating; geochemistry; Hf isotopes; geological survey engineering

About the first author: KONG Huilei, male, born in 1985, Ph.D. candidate, senior engineer, mainly engaged in the study of regional metallogeny and metallogenic regularity; E−mail: konghuilei2008@126.com.

About the corresponding author: LI Yazhi, female, born in 1979, Master, senior engineer, mainly engaged in the study of regional metallogeny and metallogenic regularity; E−mail: liyazhi2005@163.com.

Fund support: Supported by China Geological Survey Program (No.DD20190143, No.DD20160013), National Key R&D Plan (No.2019YFC0605201) and The Second Tibetan Plateau Scientific Expedition and Research(No.2019QZKK0807−02).

1 引 言

东昆仑造山带位于青藏高原东北缘,是中国中央造山带的重要组成部分,晚古生代—早中生代东昆仑处于古特提斯演化阶段(莫宣学等,2007),是形成东昆仑造山带最重要的一个阶段(罗照华等,1999),东昆仑的构造格架基本形成,是贵金属、铁、有色金属等矿产形成的重要时期,历来为研究者所重视。东昆仑古特提斯域广泛发育与俯冲−碰撞相关的岩浆作用,前人进行了大量研究,并取得了丰硕成果。然而,对于阿尼玛卿古特提斯洋俯冲作用的时限还存在争议,主要有以下几种观点:(1)古特提斯洋于晚二叠世开始俯冲(郭正府等,1998;杨经绥等,2005;莫宣学等,2007;李瑞保等,2012;李瑞保,2012;Zhang et al.,2012;Xiong et al.,2012,2013;陈国超,2014;罗明非等,2015);(2)东昆仑古特提斯洋在晚二叠世就已经关闭,三叠纪花岗岩为碰撞−碰撞后环境产物(李荣社等,2008;陈守建等,2010;Huang et al.,2014);(3)古特提斯洋俯冲起始的时间为早—中二叠世(杨延乾等,2013;Liu et al.,2014;甘彩虹,2014;熊富浩,2014;Xiong et al.,2014;Li et al.,2015;Peng et al.,2016;孔会磊等,2017a;Chen et al.,2017;Dong et al.,2018);(4)古特提斯洋俯冲一直持续到晚三叠世,三叠纪花岗岩类均为弧岩浆作用的产物(Yin and Harrison, 2000;Liu,2005;Yuan et al.,2009;Wang et al.,2011;Ding et al.,2014)。近年来,东昆仑二叠纪—三叠纪幔源岩浆事件开始受到关注,并取得了一系列成果(熊富浩等,2011a,2011b;营坤坤等,2015;奥琮等,2015;王亚磊等,2017;孔会磊等,2017a;张玉等,2017;赵旭等,2018)。然而,相对于中酸性岩,对区内镁铁−超镁铁质岩石的研究还较为薄弱,这极大制约了对东昆仑晚古生代—早中生代构造岩浆演化的研究。

因此,本文选取青海东昆仑东段察汗乌苏河地区希望沟橄榄辉长岩为研究对象,进行了详细的岩石学、地球化学、LA-ICP-MS锆石U-Pb年代学及Hf同位素研究,对其岩石成因、构造环境进行探讨,以期对东昆仑造山带古特提斯构造演化提供新的制约。

2　地质背景

东昆仑造山带位于柴达木盆地与巴颜喀拉—松潘—甘孜地体之间(图1a),是青藏高原内可与冈底斯带相媲美的另一条巨型岩浆岩带(莫宣学等,2007)。西以阿尔金走滑断裂为界与西昆仑相接,向东与秦岭—大别连接构成了中国著名的中央造山带。东昆仑造山带由东向西延伸可达1500 km(莫宣学等,2007;Dai et al., 2013),为古亚洲与特提斯构造域的交汇部位(殷鸿福等,1997),构造-岩浆活动极其发育,主要经历了早古生代原特提斯与晚古生代—早中生代古特提斯两期洋陆构造演化阶段(许志琴等,2007)。东昆仑造山带内由北往南依次发育昆北、昆中、昆南3条岩石圈大断裂,以此为界可将东昆仑划分为东昆北、东昆中、东昆南3个构造单元(姜春发等,1992,2000)(图1b)。造山带内广泛发育加里东—印支期中酸性岩类及前寒武纪变质基底。基底主要为古元古代金水口群(形成时代可约束在(2468±46)~1846 Ma,陆松年,2002;莫宣学等,2007)和小庙岩群(锆石U-Pb年龄为1683~1554Ma,陈有炘等,2011)。研究区位于东昆仑造山带东段,处于昆北与昆中断裂之间,属东昆中构造带(图1b)。从二叠纪到晚三叠世,东昆仑带产生了巨量的与俯冲-碰撞相关的岩浆作用。中酸性侵入岩主要有花岗闪长岩、石英闪长岩、二长花岗岩、英云闪长岩和正长花岗岩等(孔会磊等,2017a,2017b),基性-超基性岩体主要出露于希望沟、小尖山、拉陵高里沟脑、白日其利、中灶火、巴隆等地。

3　岩体地质及岩石学特征

希望沟镁铁质-超镁铁质杂岩体岩性主要为辉长岩、橄榄辉长岩、辉石橄榄岩、橄榄二辉岩、辉石岩等,岩浆分异较好(图2),岩石后期发生了强烈的蛇纹石化与磁铁矿化。地表露头规模较小,出露面积约2.1 km^2,形态多为不规则长条状、不规则三角形状及不规则椭圆状。杂岩体露头不好,多覆盖,北部与古元古代白沙河岩组变质岩呈断层接触,西部与晚奥陶世石英闪长岩侵入接触,东部被侏罗纪正长花岗岩侵入,南部与晚三叠世鄂拉山组呈不整合接触。杂岩体中橄榄辉石岩和橄榄辉长岩锆石U-Pb年龄分别为(262.4±1.6)Ma(孔会磊,2019)和(249.7±3.0)Ma(孔会磊等,2018),形成时代为中二叠世和早三叠世,为东昆仑晚古生代—早中生代构造旋回俯冲阶段多期次岩浆活动的产物。杂岩体

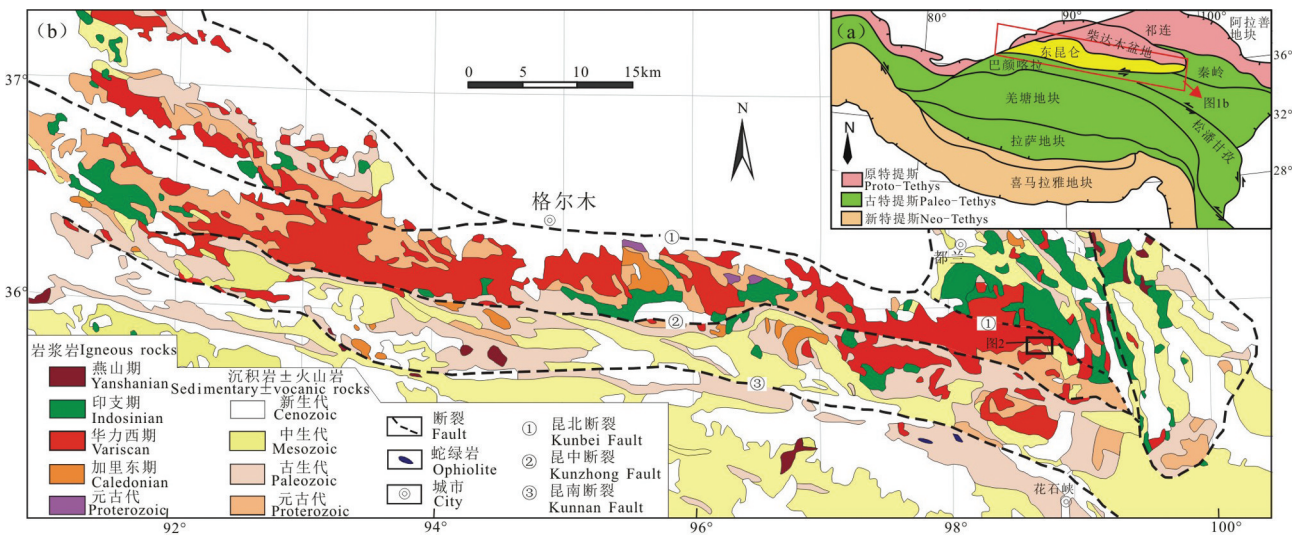

图1　东昆仑造山带构造位置(a据Xia et al., 2015b)与岩浆岩分布图(b据Xia et al., 2015a)

Fig.1　Geotectonic framework (a, after Xia et al., 2015b) and magmatite distribution (b, after Xia et al., 2015a) of East Kunlun orogenic belt

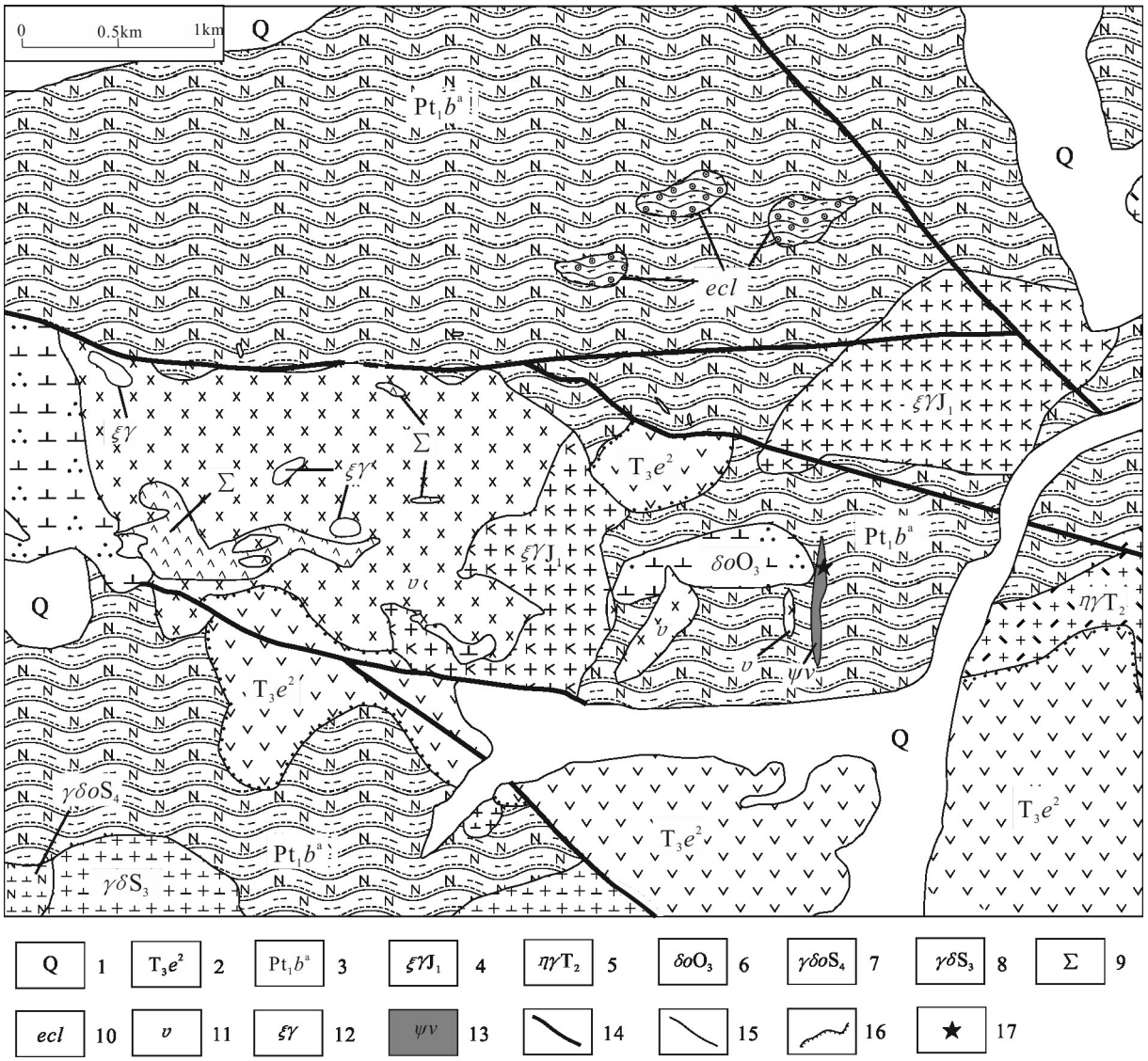

图2 希望沟一带镁铁-超镁铁质岩地质略图

1—第四系;2—上三叠统鄂拉山组英安岩段;3—古元古界白沙河组片麻岩段;4—早侏罗世正长花岗岩;5—中三叠世二长花岗岩;6—晚奥陶世石英闪长岩;7—顶志留世英云闪长岩;8—晚志留世花岗闪长岩;9—超镁铁质岩;10—榴闪岩;11—辉长岩;12—钾长花岗岩脉;13—橄榄辉长岩;14—断层;15—地质界线;16—不整合界线;17—采样位置

Fig.2 The sketch geological map of the mafic-ultramafic intrusions in Xiwanggou area

1-Quaternary; 2-Dacite member of Upper Triassic Elashan Formation; 3-Gneiss member of Paleoproterozoic Baishahe Formation; 4-Early Jurassic syenogranite; 5-Middle Triassic monzonitic granite; 6-Late Ordovician quartz diorite; 7-Top Silurian tonalite; 8-Late Silurian granodiorite; 9-Undivided ultramafic rocks; 10-Amphibole eclogite; 11-Gabbro; 12-Syenogranite vein; 13-Olivine gabbro; 14-Fault; 15-Geological boundary; 16-Unconformable boundary; 17-Sampling position

m/f比值为3.38~6.18,为铁质系列基性-超基性岩。

本文年龄及地球化学样品均采自镁铁-超镁铁质杂岩体东约1 km的橄榄辉长岩(图1b),地理坐标为35°52′51.87″N,98°42′27.43″E。岩体在平面上呈长条状南北向展布,南北长约400 m,东西宽20~30 m,侵入于古元古界金水口群白沙河组片麻岩段(图2,图3a)。岩石为灰黑色,块状构造(图3b),变余粒状结构。矿物成分主要由斜长石(>50%)、辉石(25%±)、橄榄石(20%±)及少量金属矿物(<5%)组成(图3c)。斜长石晶体呈板状,大部分晶体已次生蚀变,主要被绿泥石交代,少部分被细小闪石或绢云母交代,常呈交代残留结构。橄榄石晶体呈粒状,常沿边缘被角闪石、蛇纹石、少量滑石交代,少数呈交代残留结构(图3d),经电子探针测定为贵橄

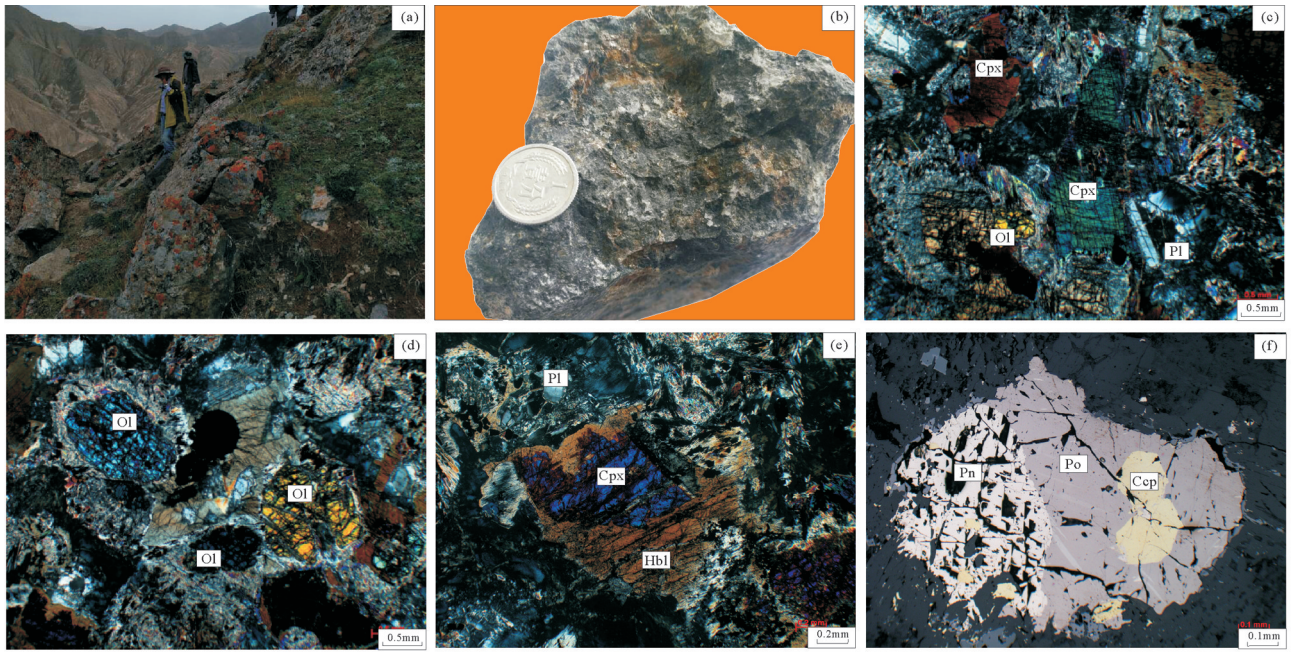

图3 希望沟橄榄辉长岩的野外露头、手标本及显微照片

a—橄榄辉长岩野外露头;b—橄榄辉长岩手标本;c—橄榄辉长岩中的橄榄石、单斜辉石、斜长石(正交偏光);d—橄榄石沿边缘被闪石、蛇纹石等交代呈残留结构(正交偏光);e—单斜辉石被角闪石交代(正交偏光);f—矿化橄榄辉长岩中的镍黄铁矿、磁黄铁矿、黄铜矿(反射光);Pl—斜长石;Ol—橄榄石;Cpx—单斜辉石;Hbl—角闪石;Pn—镍黄铁矿;Po—磁黄铁矿;Ccp—黄铜矿

Fig.3 Outcrop and hand specimen photos and microphotographs of the Xiwanggou olivine gabbro

a- Outcrop photo of olivine gabbro; b- Hand specimen photo; c- The olivine, clinopyroxene, plagioclase in olivine gabbro (crossed nicols); d- The edge of olivine altered to amphibole and serpentine, showing relict texture (crossed nicols) ; e- The clinopyroxene metasomatized by amphibole (crossed nicols); f- The pentlandite, pyrrhotite and chalcopyrite in the mineralized olivine gabbro (reflected light); Pl- Plagioclase; Ol-Olivine; Cpx-Clinopyroxene; Hbl-Hornblende; Pn-Pentlandite; Po-Pyrrhotite; Ccp-Chalcopyrite

榄石。辉石晶体多被褐色角闪石、纤维闪石或细小滑石交代,仅见少量单斜辉石残留体(图3e),电子探针测定为透辉石。金属矿物主要为磁铁矿,另可常见有磁黄铁矿、黄铜矿、镍黄铁矿在一起连生(图3f)。

4 测试分析方法

锆石的挑选、制靶、透反射光、阴极发光照相均在北京前寒武纪科技有限公司实验室进行。经过双目镜下仔细挑选表面平整光洁且具不同长宽比例、不同柱锥面特征、不同颜色的锆石颗粒,再将这些锆石黏在双面胶上,用无色透明环氧树脂固定,待环氧树脂固化之后对其表面抛光至锆石中心。在原位分析之前,通过透反射光和CL图像详细研究锆石的晶体形貌和内部结构特征,选择无明显裂痕及包裹体的锆石进行测年。锆石微量元素含量、U-Pb同位素年龄和Hf同位素测试是在中国地质调查局西安地质调查中心自然资源部岩浆作用成矿与找矿重点实验室利用7700x型四级杆等离子体质谱仪、Neptune Plus型多接收等离子体质谱仪两台仪器同时和Geolas Pro型激光剥蚀系统联机来完成的。测试束斑直径为32 μm,激光剥蚀的样品气溶胶由氦气作为载气输送到质谱仪中进行测试,为了调节和提高仪器灵敏度,气路中间引入了氩气和少量氮气。样品气溶胶经过匀化器匀化之后被分成两路,一路被输送到四极杆型等离子体质谱仪中进行锆石微量元素含量和U-Pb同位素年龄测试,另一路被输送到多接收等离子体质谱仪中进行Hf同位素测试。每分析6个点样品分析一次标准样品NIST610、91500和GJ-1,GJ-1同时作为U-Pb年龄和Hf同位素测试监控样品,本次实验GJ-1标准样品 $^{176}Hf/^{177}Hf$ 同位素的测试精准度为0.282030±20(2SD)。锆石微量元素含量和U-Pb年龄校正计算采用Glitter4.4.4来完成,Hf同位素校正计算采用实验室自己开发的计算机程序Hllow1.0来完成。详细测

试流程可参照Meng et al. (2017)。年龄计算及谐和图的绘制采用Ludwig(2003)编写的Isoplot程序。

岩石主元素、稀土元素、微量元素分析在西安地质矿产研究所实验测试中心完成,其中主元素采用荷兰帕纳科公司Axios 4.0kW顺序式X射线荧光光谱仪(XRF)进行分析,分析精度优于5%;稀土和微量元素利用美国热电公司Series Ⅱ型SX50型电感耦合等离子质谱仪(ICP-MS)进行测定,分析精度优于5%~10%。

5 测试结果

5.1 LA-ICP-MS锆石U-Pb年龄

橄榄辉长岩(17XWGUPb01)中锆石均为无色透明或浅黄色,多为短柱状及浑圆状,长轴直径为70~130 μm,长宽比为1∶1~2∶1。锆石的阴极发光图像显示部分锆石颜色偏暗,内部结构不明显,但多数锆石内部可见清晰的岩浆韵律环带(图4)。所测锆石的Th、U含量较高,分别为124.2×10^{-6}~8502.3×10^{-6}、267×10^{-6}~3878×10^{-6},Th/U比值为0.37~4.27,基本都大于0.4(表1),指示其为岩浆结晶的产物(Hoskin and Schaltegger, 2003)。一些锆石的阴极发光照片具有白色的亮边,可能为变质重结晶的结果。26个有效锆石分析点$^{206}Pb/^{238}U$表面年龄集中在270.6~256.5 Ma,落在谐和线上及其附近,其加权平均年龄为(264.9±1.2)Ma(MSWD=0.71),谐和年龄值(266.0±1.5)Ma(MSWD=0.18),二者在误差范围内基本一致(图5)。表明希望沟橄榄辉长岩结晶年龄为(264.9±1.2)Ma,属于中二叠世岩浆活动的产物。

5.2 元素地球化学

5.2.1 主量元素

5件橄榄辉长岩样品全岩地化分析数据见表2。样品的SiO_2含量变化范围较小,含量较低,为40.91%~42.14%,平均41.62%;Al_2O_3含量为6.34%~8.08%,平均值为7.09%。CaO含量为4.14%~5.05%,MgO含量较高,为28.18%~30.66%,平均为29.37%,对应的$Mg^{\#}$值为83.64~84.53,整体大于原生岩浆的$Mg^{\#}$值范围(68~75;Wilson,1989)。样品的m/f比值介于5.03~5.39,属于铁质超基性岩类。

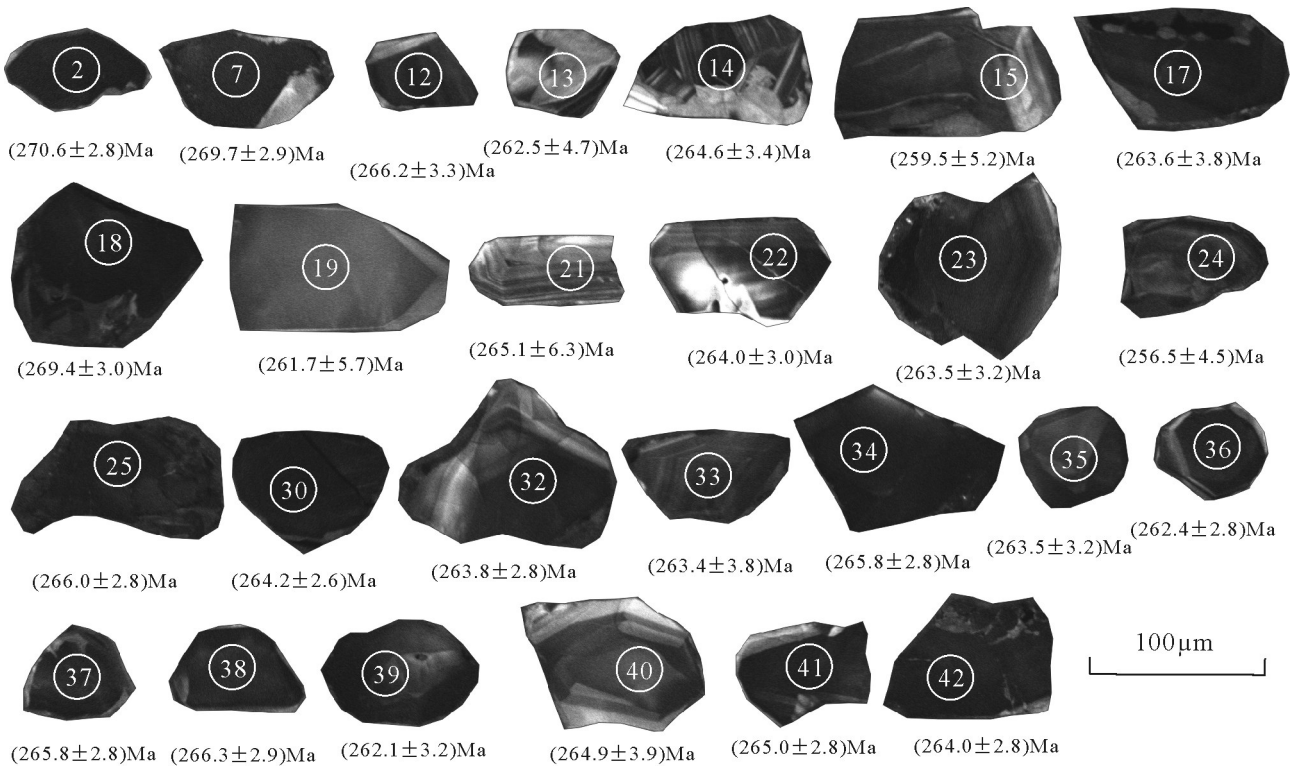

图4 希望沟橄榄辉长岩锆石阴极发光照片(圈内数字代表U-Pb分析点,其他数字代表$^{206}Pb/^{238}U$表面年龄)

Fig.4 CL images of zircons from Xiwanggou olivine gabbro (numbers in the circles represent analytical spots of U-Pb, and the values represent ages of $^{206}Pb/^{238}U$)

表1 希望沟橄榄辉长岩锆石LA-ICP-MS测年结果

Table 1 LA-ICP-MS isotopic data of zircon from Xiwanggou olivine gabbro

测点号	含量/10^{-6}			Th/U	同位素比值						年龄/Ma					
	Pb*	Th	U		$^{207}Pb/^{206}Pb$	1σ	$^{207}Pb/^{235}U$	1σ	$^{206}Pb/^{238}U$	1σ	$^{207}Pb/^{206}Pb$	1σ	$^{207}Pb/^{235}U$	1σ	$^{206}Pb/^{238}U$	1σ
2	181.9	5289.5	2395.8	2.21	0.0506	0.0008	0.2990	0.0043	0.0429	0.0005	220.9	35.3	265.6	3.4	270.6	2.8
7	129.2	3786.1	1700.0	2.23	0.0513	0.0008	0.3019	0.0046	0.0427	0.0005	252.1	37.2	267.9	3.6	269.7	2.9
12	54.1	663.8	1007.0	0.66	0.0523	0.0012	0.3037	0.0064	0.0422	0.0005	296.5	50.9	269.3	5.0	266.2	3.3
13	73.2	869.4	1373.0	0.63	0.0523	0.0020	0.2998	0.0105	0.0416	0.0008	299.0	84.0	266.2	8.2	262.5	4.7
14	45.6	473.4	881.1	0.54	0.0520	0.0012	0.3001	0.0066	0.0419	0.0005	283.7	53.5	266.5	5.2	264.6	3.4
15	30.2	632.0	500.9	1.26	0.0527	0.0024	0.2986	0.0125	0.0411	0.0008	317.5	99.7	265.3	9.8	259.5	5.2
17	223.0	8502.3	2365.3	3.59	0.0522	0.0015	0.3004	0.0079	0.0417	0.0006	294.4	63.6	266.7	6.2	263.6	3.8
18	65.9	750.4	1235.3	0.61	0.0506	0.0010	0.2977	0.0052	0.0427	0.0005	222.5	43.0	264.6	4.1	269.4	3.0
19	16.0	368.0	267.0	1.38	0.0523	0.0027	0.2987	0.0144	0.0414	0.0009	297.9	114.0	265.4	11.3	261.7	5.7
21	16.7	124.2	331.9	0.37	0.0521	0.0029	0.3017	0.0153	0.0420	0.0010	291.2	120.1	267.7	11.9	265.1	6.3
22	53.3	894.4	1171.2	0.76	0.0527	0.0010	0.3035	0.0055	0.0418	0.0005	314.6	43.6	269.1	4.3	264.0	3.0
23	91.2	3781.2	884.7	4.27	0.0531	0.0012	0.3053	0.0062	0.0417	0.0005	332.2	49.0	270.6	4.9	263.5	3.2
24	151.2	1940.8	2901.9	0.67	0.0545	0.0020	0.3047	0.0103	0.0406	0.0007	389.5	79.9	270.0	8.0	256.5	4.5
25	108.2	2184.9	1769.3	1.23	0.0520	0.0009	0.3020	0.0046	0.0421	0.0005	285.1	36.8	268.0	3.6	266.0	2.8
30	197.7	1826.5	3878.0	0.47	0.0515	0.0007	0.2972	0.0038	0.0418	0.0004	264.5	31.0	264.2	3.0	264.2	2.6
32	124.3	2342.9	2079.1	1.13	0.0519	0.0009	0.2990	0.0046	0.0418	0.0005	282.3	37.4	265.6	3.6	263.8	2.8
33	130.7	2441.6	2225.5	1.10	0.0521	0.0015	0.2995	0.0081	0.0417	0.0006	289.5	65.5	266.0	6.4	263.4	3.8
34	127.4	3492.5	1761.5	1.98	0.0512	0.0008	0.2973	0.0045	0.0421	0.0005	251.3	36.5	264.3	3.5	265.8	2.8
35	63.3	626.7	1205.5	0.52	0.0530	0.0011	0.3045	0.0061	0.0417	0.0005	326.6	48.1	269.9	4.8	263.5	3.2
36	92.7	1111.2	1741.5	0.64	0.0532	0.0009	0.3049	0.0046	0.0415	0.0005	338.8	35.9	270.2	3.6	262.4	2.8
37	114.2	2525.9	1798.9	1.40	0.0514	0.0008	0.2982	0.0046	0.0421	0.0005	258.0	37.3	265.0	3.6	265.8	2.8
38	131.6	2641.4	2122.8	1.24	0.0512	0.0009	0.2977	0.0049	0.0422	0.0005	249.6	40.2	264.6	3.8	266.3	2.9
39	55.8	520.0	1100.2	0.47	0.0530	0.0012	0.3034	0.0061	0.0415	0.0005	330.2	48.4	269.1	4.8	262.1	3.2
40	58.3	1201.6	952.0	1.26	0.0516	0.0016	0.2986	0.0084	0.0420	0.0006	269.4	67.7	265.3	6.5	264.9	3.9
41	172.9	4466.9	2537.3	1.76	0.0509	0.0008	0.2947	0.0044	0.0420	0.0005	238.1	36.6	262.2	3.5	265.0	2.8
42	124.3	3672.6	1698.3	2.16	0.0525	0.0009	0.3026	0.0048	0.0418	0.0005	306.7	37.8	268.4	3.7	264.0	2.8

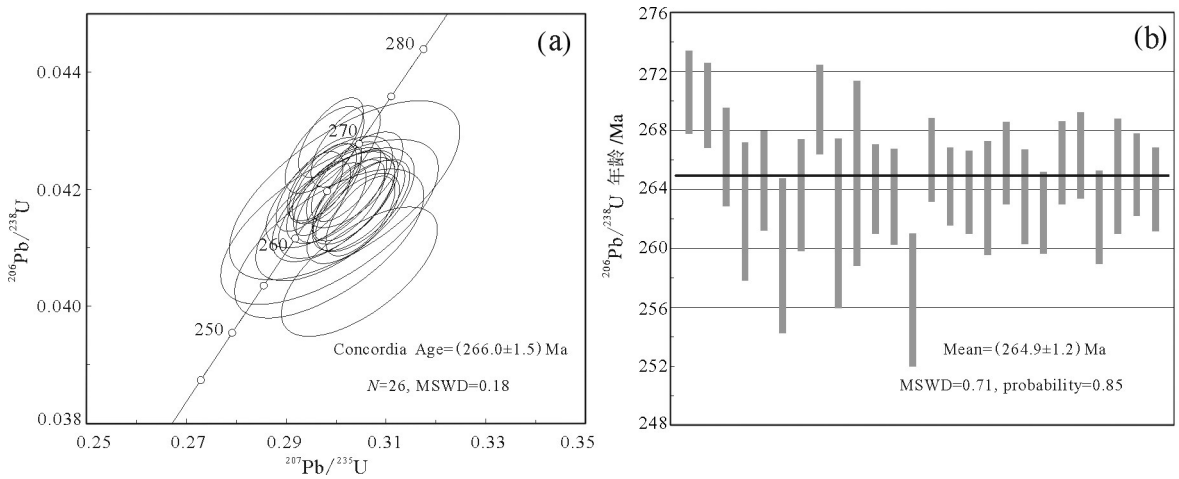

图5 希望沟橄榄辉长岩锆石U-Pb谐和图(a)和加权平均年龄图(b)

Fig.5 Zircon U-Pb concordia diagram (a) and weighted mean ages diagram (b) of Xiwanggou olivine gabbro

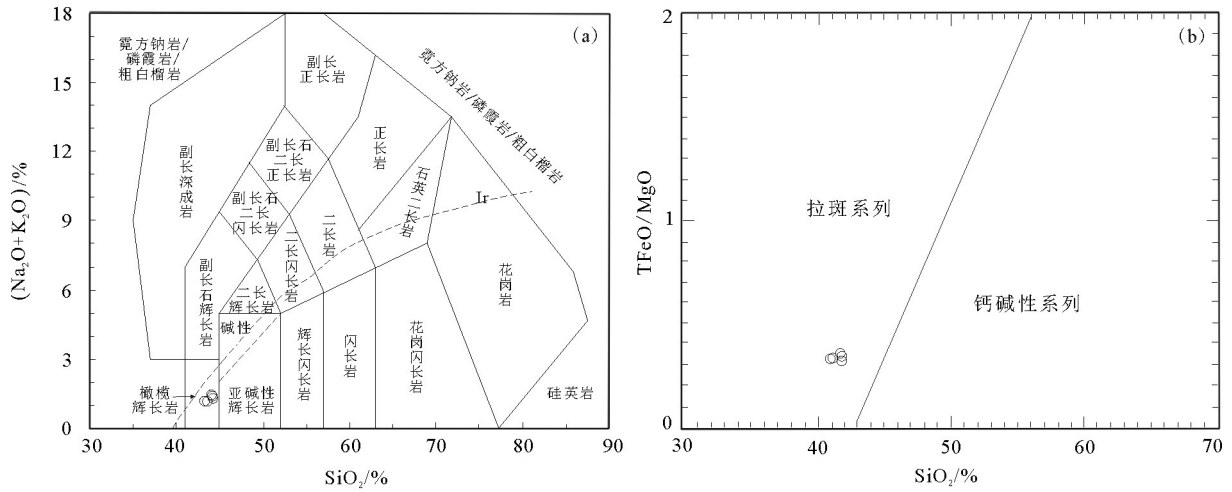

图6 希望沟橄榄辉长岩的$(K_2O+Na_2O)-SiO_2$(a据Middlemost,1994)和$TFeO/MgO-SiO_2$图解(b据Miyashiro,1974)

Fig.6 $(K_2O+Na_2O)-SiO_2$(a, after Middlemost, 1994) and $TFeO/MgO-SiO_2$ (b, after Miyashiro, 1974) plots for the Xiwanggou olivine gabbro

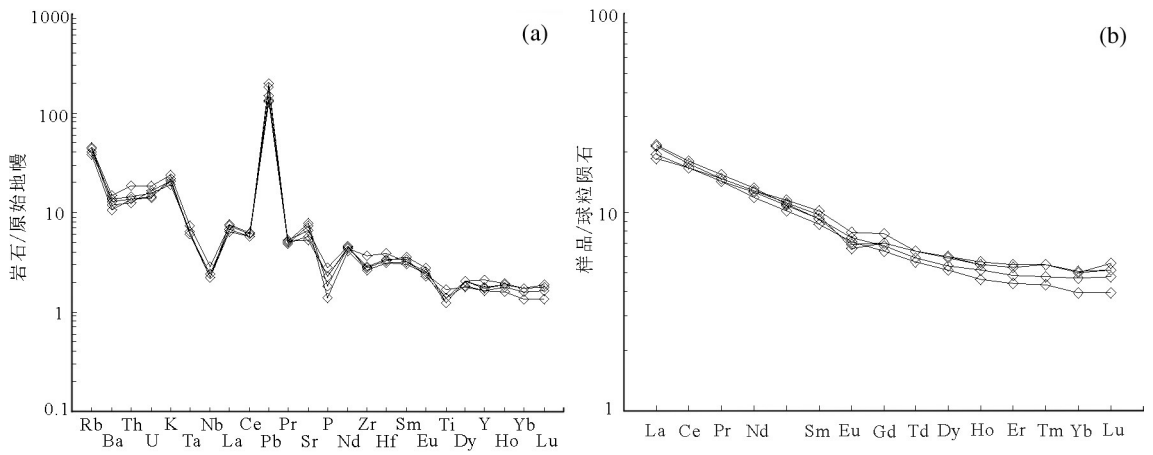

图7 希望沟橄榄辉长岩的微量元素原始地幔标准化蛛网图(a)及稀土元素球粒陨石标准化配分曲线图(b)(标准化数值据Sun and McDonough, 1989)

Fig.7 Primitive mantle-normalized trace element patterns (a) and chondrite-normalized REE patterns (b) for the olivine gabbro (normalizing values after Sun and McDonough, 1989)

样品的TiO_2含量均较低,介于0.29%~0.39%,平均值为0.32%,明显低于大洋拉斑玄武岩(2.63%)和板内玄武岩(2.23%),相对接近岛弧型玄武岩(0.98%)(Pearce,1982);P_2O_5含量较低,为0.03%~0.06%,平均值为0.05%。Na_2O含量为0.46%~0.74%,K_2O含量为0.58%~0.71%,岩石的全碱(K_2O+Na_2O)含量为1.09%~1.36%,所有岩石样品在$(Na_2O+K_2O)-SiO_2$图解中全部落在亚碱性橄榄辉长岩的范围(图6a),在$TFeO/MgO-SiO_2$图解中岩石落在拉斑系列范围内(图6b)。总体上看,希望沟橄榄辉长岩具有低硅、低钛、高镁、贫碱的特征。

5.2.2 微量和稀土元素

原始地幔标准化微量元素蛛网图(图7a)显示,橄榄辉长岩微量元素配分曲线近一致,显示了同源岩浆演化分异特征。岩石样品明显富集大离子亲石元素(LILE: Rb、Th、U、K)和Pb,相对亏损高场强元素(HFSE: Nb、P、Ti),显示具有弧岩浆的特征。

橄榄辉长岩的稀土总含量ΣREE为28.17×10^{-6}~30.95×10^{-6},平均为29.75×10^{-6}。轻重稀土比值LREE/HREE=4.32~5.06,平均为4.64,$(La/Yb)_N$为

表2 希望沟橄榄辉长岩主量元素(%)和微量元素(10^{-6})含量
Table 2 Content of major elements(%)and trace elements (10^{-6})of Xiwanggou olivine gabbro

样品号	17XWG-H1	17XWG-H2	17XWG-H3	17XWG-H4	17XWG-H5
SiO_2	41.99	42.14	41.06	42.01	40.91
TiO_2	0.29	0.39	0.32	0.32	0.29
Al_2O_3	6.90	7.75	6.34	8.08	6.37
Fe_2O_3	3.03	2.30	3.36	2.59	3.12
FeO	7.47	7.51	7.03	7.38	7.29
MnO	0.18	0.16	0.17	0.16	0.17
MgO	28.95	28.68	30.36	28.18	30.66
CaO	4.53	5.05	4.14	4.97	4.21
Na_2O	0.51	0.74	0.46	0.70	0.47
K_2O	0.71	0.62	0.66	0.58	0.62
P_2O_5	0.04	0.03	0.05	0.06	0.05
LOI	5.03	4.25	5.64	4.58	5.45
Total	99.63	99.62	99.59	99.61	99.61
$Mg^{\#}$	83.64	84.35	84.46	83.93	84.53
m/f	5.03	5.31	5.36	5.15	5.39
Sc	16.40	16.20	16.20	14.70	16.80
V	75.60	68.50	63.40	65.90	63.20
Cr	2130.00	1860.00	2020.00	2090.00	2080.00
Ni	780.00	660.00	950.00	700.00	1000.00
Co	110.00	99.00	100.00	100.00	120.00
Cu	110.00	140.00	160.00	140.00	160.00
Zn	94.30	71.80	81.30	84.70	92.90
Rb	28.50	24.30	28.80	25.40	27.90
Ba	103.00	73.10	90.50	94.60	82.50
Th	1.55	1.14	1.16	1.22	1.05
U	0.39	0.30	0.29	0.33	0.35
Ta	0.30	0.25	0.25	0.26	0.26
Nb	2.01	1.74	1.56	1.58	1.56
Pb	10.60	9.23	13.10	9.63	14.00
Sr	162.00	154.00	110.00	138.00	120.00
Zr	31.10	29.60	32.20	29.60	40.80
Hf	1.02	0.95	1.04	0.97	1.20
Y	9.55	7.33	7.92	7.47	7.99
La	5.10	4.65	4.60	5.18	4.42
Ce	10.70	10.20	10.20	11.10	10.20
Pr	1.41	1.35	1.41	1.47	1.36
Nd	6.02	5.55	6.00	6.17	5.92
Sm	1.56	1.33	1.48	1.41	1.41
Eu	0.46	0.41	0.38	0.43	0.40
Gd	1.59	1.31	1.44	1.39	1.43
Tb	0.24	0.21	0.24	0.22	0.24
Dy	1.52	1.30	1.50	1.36	1.52
Ho	0.32	0.26	0.31	0.29	0.31
Er	0.90	0.72	0.88	0.80	0.88
Tm	0.14	0.11	0.14	0.12	0.14
Yb	0.86	0.67	0.84	0.79	0.84
Lu	0.13	0.10	0.14	0.12	0.13
ΣREE	30.95	28.17	29.56	30.85	29.20
LREE/HREE	4.43	5.02	4.38	5.06	4.32
La_N/Yb_N	4.25	4.98	3.93	4.70	3.77
δEu	0.89	0.95	0.80	0.94	0.86

注:$Mg^{\#}=100\times Mg^{2+}/(Mg^{2+}+Fe^{2+})$, $m/f=(Mg^{2+}+Ni^{2+})/(Fe^{3+}+Fe^{2+}+Mn^{2+})$。

3.77~4.98,平均4.64,属轻稀土富集型。$(La/Sm)_N$为2.01~2.37,$(Gd/Yb)_N$为1.41~1.62,稀土元素配分曲线总体显示出轻稀土元素富集重稀土元素平坦的配分形式(图7b)。δEu为0.80~0.95,平均为0.89,样品显示弱的Eu负异常,表明深部岩浆房中发生了一定程度斜长石的分离结晶作用。

5.3 锆石原位Lu-Hf同位素

锆石Hf同位素分析与U-Pb测试在锆石颗粒同一位置联机同时进行。26个分析点的$^{176}Yb/^{177}Hf$和$^{176}Lu/^{177}Hf$比值范围分别为0.000981~0.090236和0.000036~0.003528(表3),除测点24、35、39外,$^{176}Lu/^{177}Hf$比值均小于0.002,表明这些锆石在形成以后,仅具有较少的放射性成因^{176}Hf的积累,因而分析获得的$^{176}Hf/^{177}Hf$比值能够代表源区的Hf同位素组成(吴福元等,2007)。26个分析点的$(^{176}Hf/^{177}Hf)_i$的变化范围在0.282709~0.283152(表3),对应的$\varepsilon_{Hf}(t)$=3.7~19.3,变化范围较大(图8a),加权平均值为12.3,数据点均落在球粒陨石Hf同位素演化线之上,更靠近亏损地幔(图8b);计算得到锆石单阶段Hf模式年龄T_{DM}为135~753 Ma,平均值为414 Ma。

6 讨　论

6.1 岩浆源区和岩石成因

一般情况下,如果锆石$\varepsilon_{Hf}(t)$为正值,说明岩浆源区为亏损地幔或从亏损地幔中新增生的年轻地壳;而$\varepsilon_{Hf}(t)$值为负值,说明源区为富集地幔或以古老地壳物质占主导(Vervoort et al., 2000; Kinny and Maas, 2003; Griffin et al., 2004)。橄榄辉长岩中锆石$^{176}Hf/^{177}Hf$比值为0.282709~0.283152,对应的$\varepsilon_{Hf}(t)$=3.7~19.3,表明岩体形成于Hf同位素亏损的地幔源区。对于幔源岩浆而言,如果锆石母岩浆直接来源于未受任何影响的亏损地幔,那么锆石结晶年龄应近似等于锆石Hf模式年龄。而橄榄辉长岩锆石单阶段Hf模式年龄T_{DM}为135~753 Ma,平均值为414 Ma,大于锆石结晶年龄265 Ma,可能是因为源区有富集岩石圈地幔的加入或遭受了地壳物质的混染(吴福元等,2007)。

希望沟橄榄辉长岩样品的Nb/Ta比值为6.00~6.96,平均为6.40,Zr/Hf比值变化于30.49~34.00,平均值为31.43,分别与大陆地壳值相近(Nb/Ta=11,

表3 希望沟橄榄辉长岩锆石Lu−Hf同位素组成

Table 3 Zircon Lu−Hf isotopic compositions of Xiwanggou olivine gabbro

测点号	t/Ma	$^{176}Yb/^{177}Hf$	$^{176}Lu/^{177}Hf$	$^{176}Hf/^{177}Hf$	2σ	$(^{176}Hf/^{177}Hf)_i$	$\varepsilon_{Hf}(t)$	2σ	T_{DM}/Ma	T^{c}_{DM}/Ma	$f_{Lu/Hf}$
2	270.6	0.005052	0.000202	0.282710	0.000074	0.282709	3.7	2.6	753	1061	-0.99
7	269.7	0.012067	0.000440	0.282792	0.000046	0.282790	6.6	1.6	643	879	-0.99
12	266.2	0.009064	0.000363	0.282805	0.000046	0.282803	6.9	1.6	624	851	-0.99
13	262.5	0.012243	0.000444	0.282913	0.000045	0.282910	10.7	1.6	475	610	-0.99
14	264.6	0.027516	0.000699	0.282834	0.000045	0.282830	7.9	1.6	589	791	-0.98
15	259.5	0.012927	0.000407	0.282908	0.000041	0.282906	10.4	1.4	481	622	-0.99
17	263.6	0.011507	0.000355	0.282854	0.000034	0.282852	8.6	1.2	556	742	-0.99
18	269.4	0.000981	0.000036	0.282998	0.000034	0.282998	13.9	1.2	351	406	-1.00
19	261.7	0.012801	0.000504	0.282858	0.000039	0.282855	8.7	1.4	552	736	-0.98
21	265.1	0.020189	0.000806	0.282741	0.000028	0.282737	4.6	1.0	721	1001	-0.98
22	264.0	0.003500	0.000123	0.282955	0.000045	0.282955	12.3	1.6	411	508	-1.00
23	263.5	0.022521	0.000733	0.282973	0.000037	0.282969	12.8	1.3	393	475	-0.98
24	256.5	0.087344	0.003204	0.282884	0.000037	0.282868	9.0	1.3	555	709	-0.90
25	266.0	0.017582	0.000572	0.282831	0.000038	0.282828	7.8	1.3	591	796	-0.98
30	264.2	0.025116	0.000860	0.283052	0.000030	0.283048	15.6	1.0	282	295	-0.97
32	263.8	0.024362	0.000807	0.282988	0.000038	0.282984	13.3	1.3	372	441	-0.98
33	263.4	0.011070	0.000404	0.283081	0.000029	0.283079	16.7	1.0	238	224	-0.99
34	265.8	0.013077	0.000434	0.283099	0.000036	0.283097	17.3	1.3	213	182	-0.99
35	263.5	0.090236	0.003528	0.283093	0.000042	0.283076	16.5	1.5	241	232	-0.89
36	262.4	0.007703	0.000288	0.283139	0.000048	0.283138	18.7	1.7	156	90	-0.99
37	265.8	0.010669	0.000502	0.283154	0.000054	0.283152	19.3	1.9	135	56	-0.98
38	266.3	0.011740	0.000412	0.283077	0.000032	0.283075	16.6	1.1	244	232	-0.99
39	262.1	0.058525	0.002280	0.283017	0.000036	0.283006	14.0	1.3	345	393	-0.93
40	264.9	0.017561	0.000591	0.283093	0.000032	0.283090	17.1	1.1	222	197	-0.98
41	265.0	0.029371	0.000986	0.283130	0.000040	0.283125	18.3	1.4	172	117	-0.97
42	264.0	0.019389	0.000610	0.282933	0.000045	0.282930	11.4	1.6	448	565	-0.98

注: $\varepsilon_{Hf}(t) = 10000 \times \{[(^{176}Hf/^{177}Hf)_S - (^{176}Lu/^{177}Hf)_S \times (e^{\lambda t} - 1)]/[(^{176}Hf/^{177}Hf)_{CHUR,0} - (^{176}Lu/^{177}Hf)_{CHUR} \times (e^{\lambda t} - 1)] - 1\}$; $T_{DM} = 1/\lambda \times \ln\{1 + [(^{176}Hf/^{177}Hf)_S - (^{176}Hf/^{177}Hf)_{DM}]/[(^{176}Lu/^{177}Hf)_S - (^{176}Lu/^{177}Hf)_{DM}]\}$; $T^{c}_{DM} = T_{DM} - (T_{DM} - t) \times [(f_{cc} - f_S)/(fc_c - f_{DM})]$; $f_{Lu/Hf} = (^{176}Lu/^{177}Hf)_S/(^{176}Lu/^{177}Hf)_{CHUR} - 1$; 其中: $\lambda = 1.867 \times 10^{-11}/a$; $(^{176}Lu/^{177}Hf)_S$ 和 $(^{176}Hf/^{177}Hf)_S$ 为样品测量值; $(^{176}Lu/^{177}Hf)_{CHUR} = 0.0332$, $(^{176}Hf/^{177}Hf)_{CHUR,0} = 0.282772$; $(^{176}Lu/^{177}Hf)_{DM} = 0.0384$, $(^{176}Hf/^{177}Hf)_{DM} = 0.28325$; $(^{176}Lu/^{177}Hf)_{平均地壳} = 0.015$; $f_{cc} = [(^{176}Lu/^{177}Hf)_{平均地壳}/(^{176}Lu/^{177}Hf)_{CHUR}] - 1$; $fs = f_{Lu/Hf}$; $f_{DM} = [(^{176}Lu/^{177}Hf)_{DM}/(^{176}Lu/^{177}Hf)_{CHUR}] - 1$; t 为锆石结晶年龄。

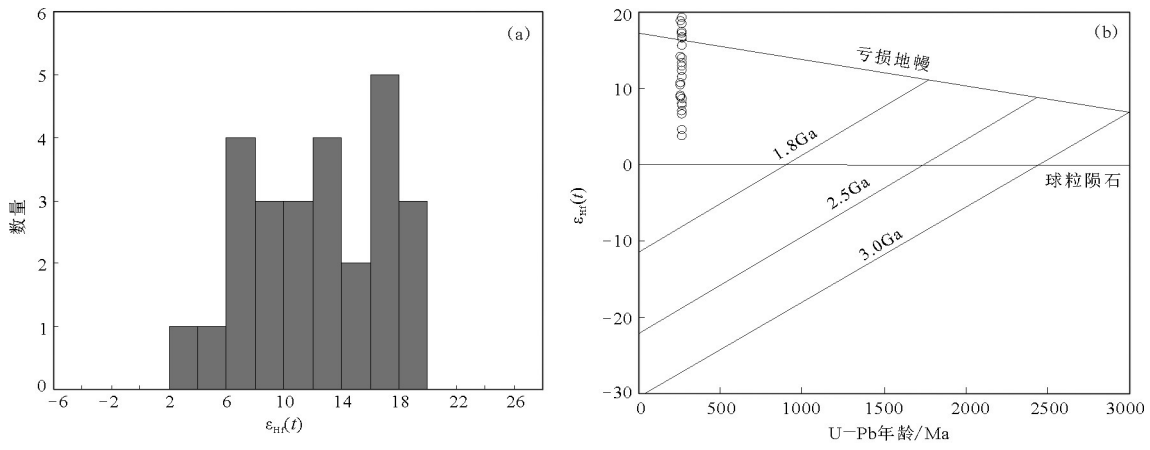

图8 希望沟橄榄辉长岩的锆石Hf同位素组成图解

Fig.8 Hf isotopic compositions of zircons from Xiwanggou olivine gabbro

Zr/Hf=33,据Taylor and McLennan,1985),而低于洋中脊玄武岩值(Nb/Ta=17.7,Zr/Hf=36.1,据Sun and McDonough,1989),反映橄榄辉长岩受到地壳同化混染的影响。地壳中Ce/Pb比值<15,而典型地幔Ce/Pb=25±5(Hofmann et al., 1986)。希望沟橄榄辉长岩中Ce/Pb比值为0.73~1.15,明确显示岩体受到同化混染作用;Nb/U比值可作为判别地壳混染的标志,洋中脊玄武岩和洋岛玄武岩Nb/U比值为47±10,而大陆地壳和原始地幔Nb/U平均值分别为8.93和33.59(Taylor and McLennan,1985),希望沟橄榄辉长岩Nb/U比值在4.46~5.80,远离原始地幔平均值,接近大陆地壳,反映岩浆在上升过程中有陆壳物质的加入。

希望沟橄榄辉长岩样品Th/Yb比值为1.25~1.80,在Th/Yb-Nb/Yb图解中投点均明显偏离MORB-OIB演化线(图9a),暗示其形成明显受到俯冲组分的影响(Pearce and Peate,1995)。在Nb/Zr-Th/Zr图解中,样品显示了流体俯冲交代的趋势(图9b)。以上特征可看出有含水流体进入地幔源区(Woodhead et al., 2001),这种岩石圈地幔主要是由早期大洋俯冲阶段流体交代形成。综上所述,希望沟橄榄辉长岩源区主要为亏损地幔,可能有早期流体交代的岩石圈地幔组分的加入,并经历了地壳物质的混染。

6.2 希望沟橄榄辉长岩形成时代及其构造意义

希望沟橄榄辉长岩明显富集大离子亲石元素(Rb、Th、U、K)和Pb,相对亏损高场强元素(Nb、P、Ti),显示了岛弧岩浆岩的特征。样品的TiO_2含量均较低,介于0.29%~0.39%,相对接近岛弧型玄武岩(0.98%),明显低于洋中脊玄武岩(1.5%)和洋岛玄武岩(大于2.0%)(Pearce,1982);样品的微量元素Nb/La=0.31~0.39(<1),La/Ta=17.00~19.92(>15),Th/Yb=1.25~1.80(>0.1),Th/Nb=0.66~0.77(>0.07),进一步显示了岛弧的性质(Condie,1989)。

为进一步探讨橄榄辉长岩的构造环境,笔者利用不活动元素协变关系进行构造环境判别。在Nb×2-Zr/4-Y图解(图10a)中,岩石表现出火山弧玄武岩的特征;在Zr/117-Th-Nb/16判别图(图10b)中,样品均落在破坏板块边缘玄武岩区域,暗示橄榄辉长岩为俯冲作用形成的岛弧岩浆岩。

东昆仑造山带发育巨量与俯冲-碰撞相关的岩浆活动,前人进行了大量研究工作,然而,对于阿尼玛卿古特提斯洋俯冲作用起始的时限还存在争议。有学者认为古特提斯洋于晚二叠世开始俯冲,闭合于中三叠世,晚二叠世—中三叠世早期为俯冲造山阶段(260~238 Ma),中三叠世晚期—晚三叠世早期为同碰撞阶段(237~230 Ma)(郭正府等,1998;杨经绥等,2005;莫宣学等,2007;李瑞保等,2012;李瑞保,2012;Zhang et al., 2012;Xiong et al., 2012,2013;陈国超,2014;罗明非等,2015)。也有学者认为古特提斯洋俯冲起始的时间可能早于260 Ma,杨延乾等(2013)认为古特提斯洋268 Ma左右就已经进入俯冲阶段;Liu et al.(2014)获得小庙镁铁质岩墙群角闪石Ar-Ar年龄为(277.76±2.72)Ma,认为阿

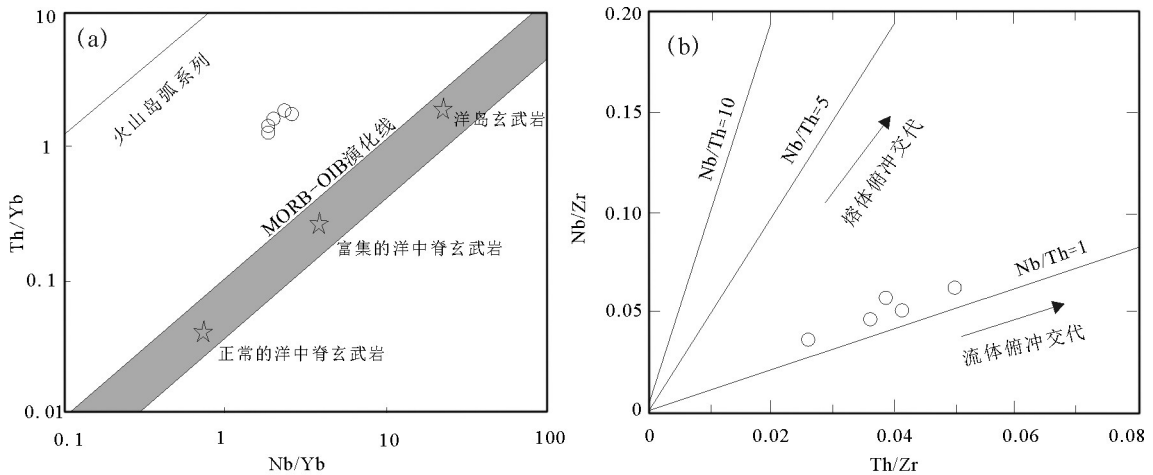

图9 希望沟橄榄辉长岩源区性质判别图解(a据Pearce, 2008;b据Woodhead et al., 2001)

Fig.9 Discrimination diagram of the source characteristics for Xiwanggou olivine gabbro (a, after Pearce, 2008; b, after Woodhead et al., 2001)

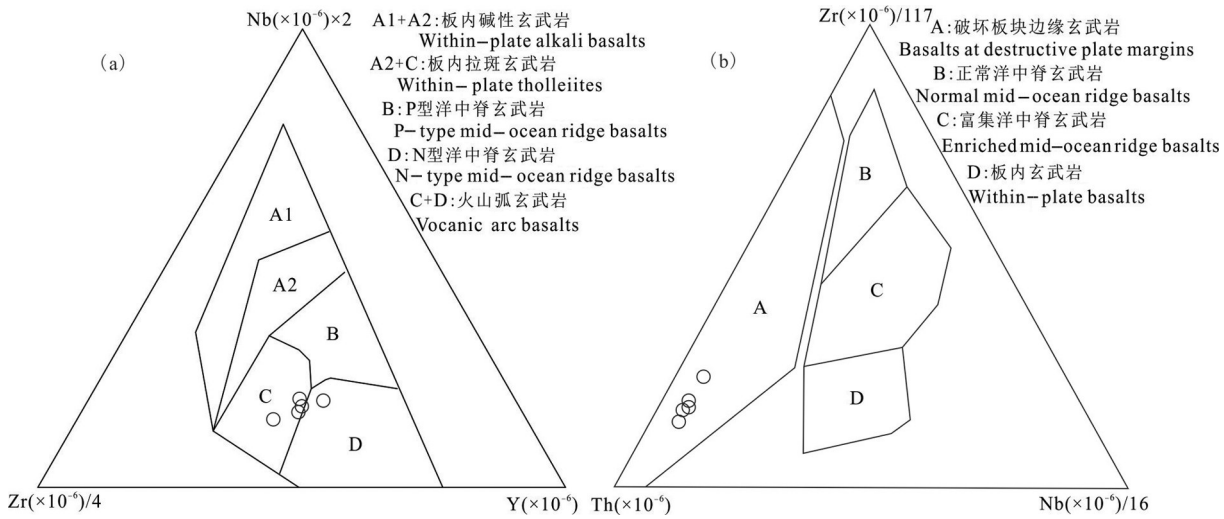

图10 希望沟橄榄辉长岩构造环境判别图解(a据Meschede, 1986;b据Wood et al., 1979)

Fig.10 Tectonic discrimination diagrams for Xiwanggou olivine gabbro (a, after Meschede, 1986; b, after Wood et al., 1979)

尼玛卿古特提斯洋北向俯冲的起始时间不晚于278 Ma;随后其他一些学者也相继提出了古特提斯洋俯冲开始于早二叠世的观点(熊富浩,2014;Xiong et al., 2014;Li et al., 2015;Peng et al., 2016;Chen et al., 2017;陈邦学等,2019)。一般认为,中晚三叠世具有典型磨拉石堆积特征的不整合面是阿尼玛卿大洋闭合的标志,东昆仑阿尼玛卿洋闭合时限接近晚三叠世,晚三叠世之后东昆仑进入碰撞后伸展阶段(230~185 Ma)(熊富浩,2014)。

晚古生代—早中生代是东昆仑构造演化的一个重要阶段,近年来,东昆仑二叠纪—三叠纪幔源岩浆事件逐渐受到研究者重视,为古特提斯构造演化研究提供了新的方向。熊富浩等(2011a)获得白日其利角闪辉长岩的锆石U-Pb年龄为(248.9±4.2) Ma,认为是早三叠世阿尼玛卿古特提斯洋俯冲阶段岩浆活动的产物。熊富浩等(2011b)与菅坤坤等(2015)分别对白日其利及中灶火镁铁质岩墙群进行了研究,获得年龄分别为(251±2)Ma与(249±1) Ma,认为是俯冲环境中弧后伸展作用影响下板片流体交代富集地幔的产物。奥琮等(2015)获得小尖山中细粒辉长岩的锆石U-Pb年龄为(227.8±0.9) Ma,认为形成于造山后伸展环境。孔会磊等(2017a)对位于希望沟西北的加当辉长岩进行了研究,获得其结晶年龄为(262.5±2.5)Ma,认为是古特提斯洋北向俯冲的产物。张玉等(2017)和赵旭等(2018)分别获得阿拉思木辉长岩及按纳格角闪辉长岩锆石U-Pb年龄为(241.1±1.2)Ma与(242±2)Ma,均代表了东昆仑洋壳俯冲的晚期记录。Xiong et al.(2012)获得巴隆地区瑙木浑花岗闪长岩体中MME结晶年龄为(263±2)Ma,认为其形成于俯冲环境。从上可以看出,东昆仑二叠纪—三叠纪幔源岩浆活动主体形成于古特提斯洋俯冲阶段,少部分形成于后碰撞伸展阶段。

本文获得希望沟橄榄辉长岩的加权平均年龄为(264.9±1.2)Ma,表明岩体形成时代为中二叠世,同时结合前文岩石成因及构造环境分析,笔者认为希望沟橄榄辉长岩为阿尼玛卿古特提斯洋俯冲阶段的产物,说明至少在中二叠世265 Ma古特提斯洋就开始北向俯冲,这为东昆仑古特提斯构造演化提供了新的年代学证据,并进一步印证了东昆仑造山带广泛发育的二叠纪—三叠纪幔源岩浆事件。

7 结 论

(1)岩石地球化学特征表明,希望沟橄榄辉长岩具有低硅、低钛、高镁、贫碱的特征,属亚碱性系列岩石。岩石富集LILE(Rb、Th、U、K)和Pb,相对亏损HFSE(Nb、P、Ti),显示轻稀土富集的特征,具有弱的Eu负异常。

(2)橄榄辉长岩锆石$^{176}Hf/^{177}Hf$比值为0.282709~0.283152,对应的$\varepsilon_{Hf}(t)$=3.7~19.3。研究认为其源区主要为亏损地幔,可能有早期流体交代的岩石圈地幔组分的加入,并经历了地壳物质的混染。

(3)本文获得希望沟橄榄辉长岩LA-ICP-MS锆石U-Pb年龄为(264.9±1.2)Ma,形成于中二叠世,结合东昆仑区域构造演化,认为是阿尼玛卿古特提斯洋俯冲阶段的产物,说明古特提斯洋在中二叠世已北向俯冲。

致谢:薄片鉴定过程中得到了中国地质调查局西安地质调查中心叶芳研究员的指导,锆石U-Pb年龄和Hf同位素测试及数据处理得到自然资源部岩浆作用成矿与找矿重点实验室李艳广工程师、靳梦琪工程师的热心帮助,文稿修改过程中审稿专家提出了宝贵的修改意见,在此一并表示衷心的感谢。

References

Ao Cong, Sun Fengyue, Li Bile, Wang Guan, Li Liang, Li Shijin, Zhao Junwei. 2015. U-Pb dating, geochemistry and tectonic implication of Xiaojianshan gabbro in Qimantage Mountain, Eastern Kunlun oregenic belt[J]. Geotectonica et Metallogenia, 39(6): 1176-1184 (in Chinese with English abstract).

Chen Bangxue, Xu Shengli, Yang Yousheng, Zhou Nengwu, Zhu Zhixin. 2019. Genesis and tectonic significance of Late Permian Qimulaike intrusive rocks in the west of East Kunlun Mountains, Xinjiang[J]. Geological Bulletin of China, 38(6):1040-1051(in Chinese with English abstract).

Chen G C, Pei X Z, Li R B, Li Z C, Liu C J, Chen Y X, Pei L, Wang M, Li X B. 2017. Paleo-Tethyan oceanic crust subduction in the eastern section of the East Kunlun Orogenic Belt: Geochronology and petrogenesis of the Qushi'ang granodiorite[J]. Acta Geologica Sinica, 91(2): 565-580.

Chen Guochao. 2014. Petrology, Genesis and Geological Significance of Late Paleozoic- Early Mesozoic Granitoids in East Kunlun Orogen[D]. Xi'an: Chang'an University(in Chinese with English abstract).

Chen Shoujian, Li Rongshe, Ji Wenhua, Zhao Zhenming, Liu Rongli, Jia Baohua, Zhang Zhenfu, Wang Guocan. 2010. The Permian lithofacies paleogeographic characteristics and basin- mountain conversion in the Kunlun orogenic belt[J]. Geology in China, 37 (2): 374-393(in Chinese with English abstract).

Chen Youxin, Pei Xianzhi, Li Ruibao, Liu Zhanqing, Li Zuochen, Zhang Xiaofei, Chen Guochao, Liu Zhigang, Ding Saping, Guo Junfeng. 2011. Zircon U- Pb age of Xiaomiao formation of proterozoic in the eastern section of the East Kunlun Orogenic Belt[J]. Geoscience, 25(3): 510-521(in Chinese with English Abstract).

Condie K C. 1989. Geochemical changes in basalts and andesites across the Archean- Proterozoic boundary: Identification and significance[J]. Lithos, 23(1): 1-18.

Dai J G, Wang C S, Hourigan J, Santosh M. 2013. Multi- stage tectono-magmatic events of the Eastern Kunlun Range, northern Tibet: insights from U- Pb geochronology and(U- Th)/He thermochronology[J]. Tectonophysics, 599: 97-106.

Ding Q F, Jiang S Y, Sun F Y. 2014. Zircon U-Pb geochronology, geochemical and Sr-Nd-Hf isotopic compositions of the Triassic granite and diorite dikes from the Wulonggou mining area in the Eastern Kunlun Orogen, NW China: Petrogenesis and tectonic implications[J]. Lithos, 205(9): 266-283.

Dong Y P, He D F, Sun S S, Liu X M, Zhou X H, Zhang F F, Yang Z, Cheng B, Zhao G C, Li J H. 2018. Subduction and accretionary tectonics of the East Kunlun orogen, western segment of the Central China Orogenic System[J]. Earth-Science Reviews, 186, 231-261.

Gan Caihong. 2014. Petrology, Geochemistry, U-Pb Dating and Hf Isotopic Composition of Zircons in Igneous Rocks from East Kunlun Orogen, Qinghai[D]. Beijing: China University of Geosciences(Beijing)(in Chinese with English abstract).

Griffin WL, Belousova E A, Shee S R. 2004. Crustal evolution in the northern Yilarm Craton: U- Pb and Hf- isotope evidence from detrital zircons[J]. Precambrian Research, 131(3/4): 231-282.

Guo Zhengfu, Deng Jinfu, Xu Zhiqin, Mo Xuanxue, Luo Zhaohua. 1998. Late Paleozoic-Mesozoic intracontinental orogenic process and intermediate- acidic igneous rocks from the Eastern Kunlun Mountains of Northwestern China[J]. Geoscience, 12(3): 344-352 (in Chinese with English abstract).

Hofmann A W, Jochum K P, Seufert M, White W M. 1986. Nb and Pb in oceanic basalts: New constraints on mantle evolution[J]. Earth and Planetary Science Letters, 79(1/2): 33-45.

Hoskin P W O, Schaltegger U. 2003. The composition of zircon and igneous and metamorphic petrogenesis[J]. Reviews in Mineralogy and Geochemistry, 53: 27-55.

Huang H, Niu Y L, Nowell G, Zhao Z D, Yu X H, Zhu D C, Mo X X, Ding S. 2014. Geochemical constraints on the petrogenesis of granitoids in the East Kunlun Orogenic belt, northern Tibetan Plateau: Implications for continental crust growth through syncollisional felsic magmatism[J]. Chemical Geology, 370: 1-18.

Jian Kunkun, Wei Yanxia, Shi Bin, Liu Li, Wang Xing, Yuan Zhang. 2015. Petrogenesis and geological significance of the Early Mesozoic mafic dyke swarms in Zhongzaohuo area, East Kunlun orogenic belt[J]. Geology in China, 42(5): 1457-1470(in Chinese with English abstract).

Jiang Chunfa, Wang Zongqi, Li Jinyi. 2000. Opening- closing Tectonics of the Central Orogenic Belt[M]. Beijing: Geological Publishing House: 1-54(in Chinese with English abstract).

Jiang Chunfa, Yang Jingsui, Feng Binggui, Zhu Zhizhi, Zhao Min, Chai Yaowu, Shi Xide, Wang Huaida, Hu Jinqing. 1992. Opening-closing Tectonics of Kunlun Mountains[M]. Beijing: Geological Publishing House: 183-217(in Chinese with English abstract).

Kinny P D and Maas R. 2003. Lu-Hf and Sm-Nd isotope systems in zircon[J]. Reviews in Mineralogy and Geochemistry, 53(1):327-341.

Kong Huilei, Li Jinchao, Li Yazhi, Jia Qunzi, Guo Xianzheng. 2017a. Zircon LA−ICP−MS U−Pb dating and its geological significance of the Jiadang gabbro in the eastern section of East Kunlun, Qinghai Province[J]. Geology and Exploration, 53(5): 889−902(in Chinese with English abstract).

Kong Huilei, Li Jinchao, Li Yazhi, Jia Qunzi, Guo Xianzheng, Wang Yu. 2017b. Zircon LA−ICP−MS U−Pb dating and its geological significance of the Halongxiuma pyroxene peridotite in East Kunlun, Qinghai Province[J]. Geological Science and Technology Information, 36(1): 41−47(in Chinese with English abstract).

Kong Huilei, Li Jinchao, Li Yazhi, Jia Qunzi, Guo Xianzheng, Zhang Bin. 2018. Zircon U− Pb dating, geochemistry and geological significance of the Jiadang olivine gabbro in the eastern section of East Kunlun, Qinghai Province[J]. Acta Geologica Sinica, 92(5): 964−978(in Chinese with English abstract).

Kong Huilei, Li Yazhi, Li Jinchao, Jia Qunzi, Guo Xianzheng, Zhang Bin. 2019. LA− ICP− MS zircon U− Pb dating and geochemical characteristics of the Xiwanggou olivine pyroxenolite in East Kunlun[J]. Journal of Geomechanics, 25(3): 440−452(in Chinese with English abstract).

Li Rongshe, Ji Wenhua, Yang Yongcheng, Yu Pusheng, Zhao Zhenming, Chen Shoujian, Meng Yong, Pan Xiaoping, Shi Bingde, Zhang Weiji, Li Hang, Luo Changyi. 2008. Geology of Kunlun Mountains and Adjacent Areas[M]. Beijing: Geological Publishing House: 1−400(in Chinese).

Li Ruibao, Pei Xianzhi, Li Zuochen, Liu Zhanqing, Chen Guochao, Chen Youxin, Wei Fanghui, Gao Jingmin, Liu Chenjun, Pei Lei. 2012. Geological characteristics of Late Paleozoic− Mesozoic unconformities and their response to some significant tectonic events in eastern part of Eastern Kunlun[J]. Earth Science Frontiers, 19(5): 244−254(in Chinese with English abstract).

Li Ruibao. 2012. Research on the Late Paleozoic− Early Mesozoic Orogeny in East Kunlun Orogen[D]. Xi'an: Chang'an University (in Chinese with English abstract).

Li X W, Huang X F, Luo M F, Dong G C, Mo X X. 2015. Petrogenesis and geodynamic implications of the Mid−Triassic lavas from East Kunlun, northern Tibetan Plateau[J]. Journal of Asian Earth Sciences, 105: 32−47.

Liu B, Ma C Q, Zhang J Y, Xiong F H, Huang J, Jiang H A. 2014. $^{40}Ar-^{39}Ar$ age and geochemistry of subduction−related mafic dikes in northern Tibet, China: petrogenesis and tectonic implications[J]. International Geology Review, 56: 57−73.

Liu H T. 2005. Petrology, geochemistry and geochronology of late Triassic volcanics, Kunlun orogenic belt, western China: Implications for tectonic setting and petrogenesis[J]. Geochemical Journal, 39(1): 1−20.

Lu Songnian. 2002. Preliminary Study of Precambrian Geology in the North Tibet− Qinghai Plateau[M]. Beijing: Geological Publishing House, 1−125(in Chinese with English abstract).

Ludwig K R. 2003. Users Manual for Isoplot 3.00: A Geochronological Toolkit for Microsoft Excel[M]. Berkeley: Berkeley Geochronology Center Special Publication, 25−32.

Luo Mingfei, Mo Xuanxue, Yu Xuehui, Li Xiaowei, Huang Xiongfei. 2015. Zircon U−Pb geochronology, petrogenesis and implications of the Later Permian granodiorite from the Wulonggou area in East Kunlun, Qinghai Province[J]. Earth Science Frontiers, 22(5): 182−195(in Chinese with English abstract).

Luo Zhaohua, Deng Jinfu, Cao Yongqing, Guo Zhengfu, Mo Xuanxue. 1999. On Late Paleozoic− Early Mesozoic volcanism and regional tectonic evolution of eastern Kunlun, Qinghai Province[J]. Geoscience, 13(1): 51−56(in Chinese with English abstract).

Meng E, Wang C Y, Li Y G, Li Z, Yang H, Cai J, Ji L, Jin M Q. 2017. Zircon U−Pb−Hf isotopic and whole−rock geochemical studies of Paleoproterozoic metasedimentary rocks in the northern segment of the Jiao− Liao− Ji Belt, China: Implications for provenance and regional tectonic evolution[J]. Precambrian Research, 298: 472−489.

Meschede M. 1986. A method of discriminating between different types of mid−ocean ridge basalts and continental tholeiites with the Nb−Zr−Y diagram[J]. Chemical Geology, 56(3/4): 207−218.

Middlemost E A K. 1994. Naming materials in the magma/igneous rock system[J]. Earth−Science Reviews, 37(3/4): 215−224.

Miyashiro A. 1974. Volcanic rock series in island arcs and active continental margins[J]. American Journal of Science, 274(4): 321−355.

Mo Xuanxue, Luo Zhaohua, Deng Jinfu, Yu Xuehui, Liu Chengdong, Chen Hongwei, Yuan Wanming, Liu Yunhua. 2007. Granitoids and crustal growth in the East− Kunlun Orogenic Belt[J]. Geological Journal of China Universities, 13(3): 403− 414(in Chinese with English abstract).

Pearce J A and Peate D W. 1995. Tectonic implications of the composition of volcanic arc magmas[J]. Annual Review of Earth and Planetary Sciences, 23(1): 251−285.

Pearce J A. 1982. Trace element characteristics of lavas from destructive plate boundaries[C]// Thorpe R S(ed.). Andesites: Orogenic Andesites and Related Rocks. Chichester: Willy: 525−548.

Pearce J A. 2008. Geochemical fingerprinting of oceanic basalts with applications to ophiolite classification and the search for Archean oceanic crust[J]. Lithos, 100(1/4): 14−48.

Peng B, Li B L, Zhao T F, Wang C, Chang J J, Wang G Z, Yang W L. 2016. Identification of A−type granite in the southeastern Kunlun Orogen, Qinghai Province, China: implications for the tectonic framework of the Eastern Kunlun Orogen[J]. Geological Journal, 52 (3): 454−469.

Sun S S and McDonough W F. 1989. Chemical and isotopic systematics of oceanic basalt: Implications for mantle composition and process[C]//Saunders A D, Norry M J(eds.). Magmatism in the Ocean Basins. Geological Society, London, Special Publication,

42: 313−345.

Taylor S R, McLennan S M. 1985. The Continental Crust: Its Composition and Evolution[M]. Oxford: Blackwell Scientific Publications, 57−72.

Vervoort J D, Pachelt P J, Albarede F, Blichert− Toft J, Rudnick R, Downes H. 2000. Hf− Nd isotopic evolution of the lower crust[J]. Earth and Planerary Science Letters, 181: 115−129.

Wang Q, Li Z X, Chung S L, Wyman D A, Sun Y L, Zhao Z H, Zhu Y T, Qiu H N. 2011. Late Triassic high− Mg andesite/dacite suites from northern Hohxil, North Tibet: Geochronology, geochemical characteristics, petrogenetic processes and tectonic implications[J]. Lithos, 126: 54−67.

Wang Yalei, Zhang Zhaowei, Zhang Jiangwei, Qian Bing, Liu Yuegao, You Minxin. 2017. Early Mesozoic mantle− derived magmatic events and their geological significance in the East Kunlun orogenic belt[J]. Geology and Exploration, 53(5): 855− 866(in Chinese with English abstract).

Wilson M. 1989. Igneous Petrogenesis: A Global Tectonic Approach[M]. London: Unwin Hyman, 1−466.

Wood D A, Joron J L, Treuil M. 1979. A re− appraisal of the use of trace elements to classify and discriminate between magma series erupted in different tectonic settings[J]. Earth and Planetary Science Letters, 45(2): 326−336.

Woodhead J D, Hergt J M, Davidson J P, Eggins S M. 2001. Hafnium isotope evidence for conservative element mobility during subduction zone process[J]. Earth and Planetary Science Letters, 192(3): 331−346.

Wu Fuyuan, Li Xianhua, Zheng Yongfei, Gao Shan. 2007. Lu− Hf isotopic systematics and their applications in petrology[J]. Acta Petrologica Sinica, 23(2): 185−220(in Chinese with English abstract).

Xia R, Wang C M, Qing M, Deng J, Carranza E J M, Li W L, Guo X D, Ge L S, Yu W Q. 2015a. Molybdenite Re− Os, zircon U− Pb dating and Hf isotopic analysis of the Shuangqing Fe−Pb−Zn−Cu skarn deposit, East Kunlun Mountains, Qinghai Province, China[J]. Ore Geology Reviews, 66: 114−131.

Xia R, Wang C M, Qing M, Li W L, Carranza E J M, Guo X D, Ge L S, Zeng G Z. 2015b. Zircon U−Pb dating, geochemistry and Sr−Nd−Pb−Hf−O isotopes for the Nan'getan granodiorites and mafic microgranular enclaves in the East Kunlun Orogen: Record of closure of the Paleo−Tethys[J]. Lithos, 234: 47−60.

Xiong F H, Ma C Q, Jiang H A, Liu B, Zhang J Y, Zhou Q. 2013. Petrogenetic and tectonic significance of Permian calc− alkaline lamprophyres, East Kunlun orogenic belt, Northern Qinghai−Tibet Plateau[J]. International Geology Review, 55: 1817−1834.

Xiong F H, Ma C Q, Zhang J Y, Liu B, Jiang H A. 2014. Reworking of old continental lithosphere: an important crustal evolution mechanism in orogenic belts, as evidenced by Triassic I− type granitoids in the East Kunlun orogen, Northern Tibetan Plateau[J]. Journal of the Geological Society, 171: 847−863.

Xiong F H, Ma C Q, Zhang J Y, Liu B. 2012. The origin of mafic microgranular enclaves and their host granodiorites from East Kunlun, Northern Qinghai− Tibet Plateau: implications for magma mixing during subduction of Paleo− Tethyan lithosphere[J]. Mineralogy and Petrology, 104: 211−224.

Xiong Fuhao, Ma Changqian, Zhang Jinyang, Liu Bin, Jiang Hongan, Huang Jian. 2011b. Zircon LA−ICP−MS U−Pb dating of Bairiqili gabbro pluton in the East Kunlun Orogenic Belt and its geological significance[J]. Geological Bulletin of China, 30(8): 1196−1202(in Chinese with English abstract).

Xiong Fuhao, Ma Changqian, Zhang Jinyang, Liu Bin. 2011a. LA− ICP− MS zircon U− Pb dating, elements and Sr− Nd− Hf isotope geochemistry of the Early Mesozoic mafic dyke swarms in East Kunlun Orogenic Belt[J]. Acta Petrologica Sinica, 27(11): 3350− 3364(in Chinese with English abstract).

Xiong Fuhao. 2014. Spatial− temporal Pattern, Petrogenesis and Geological Implications of Paleo− Tethyan Granitoids in the East Kunlun Orogenic Belt(Eastern Segment) [D]. Wuhan: China University of Geoscience, 22−74(in Chinese with English abstract).

Xu Zhiqin, Yang Jingsui, Li Haibing, Zhang Jianxin, Wu Cailai. 2007. Orogenic Palteaux: Terrane Aamalgamation, Collision and Uplift in the Qinghai− Tibet Plateau[M]. Beijing: Geological Publishing House, 1−458(in Chinese with English abstract).

Yang Jingsui, Xu Zhiqin, Li Haibing, Shi Rendeng. 2005. The paleo− Tethyan volcanism and plate tectonic regime in the A'nyemaqen region of East Kunlun, northern Tibet Plateau[J]. Acta Petrologica et Mineralogica, 24(5): 369−380(in Chinese with English abstract).

Yang Yanqian, Li Bile, Xu Qinglin, Zhang Bingshe. 2013. Zircon U− Pb ages and its geological significance of the monzonitic granite in the Aikengdelesite, Eastern Kunlun[J]. Northwestern Geology, 46 (1): 56−62(in Chinese with English abstract).

Yin A, Harrison TM. 2000. Geologic evolution of the Himalayan− Tibetan orogen[J]. Annual Review of Earth and Planetary Sciences, 28: 211−280.

Yin Hongfu, Zhang Kexin. 1997. Characteristics of the eastern Kunlun orogenic belt[J]. Earth Science: Journal of China University of Geosciences, 22(4): 339−342(in Chinese with English abstract).

Yuan C, Sun M, Xiao W J, Wilde S, Li X H, Liu X H, Long X P, Xia X P, Ye K, Li J L. 2009. Garnet−bearing tonalitic porphyry from East Kunlun, northeast Tibetan plateau: Implications for adakite and magmas from the mash zone[J]. International Journal of Earth Sciences, 98: 1489−1510.

Zhang J Y, Ma C Q, Xiong F H, Liu B. 2012. Petrogenesis and tectonic significance of the Late Permian− Middle Triassic calc− alkaline granites in the Balong region, eastern Kunlun Orogen, China[J]. Geological Magazine, 149(5): 892−908.

Zhang Yu, Pei Xianzhi, Li Ruibao, Liu Chengjun, Chen Youxin, Li Zuochen, Wang Xing, Hu Chenguang, Yan Quanzhi, Peng Sizhong. 2017. Zircon U− Pb geochronology, geochemistry of the Alasimu

gabbro in eastern section of East Kunlun Mountains and the closing time of Paleo-ocean basin[J]. Geology in China, 44(3): 526-540 (in Chinese with English abstract).

Zhao Xu, Fu Lebing, Wei Junhao, Zhao Yujing, Tang Yang, Yang Baorong, Guan Bo, Wang Xiaoyun. 2018. Geochemical characteristics of Annage hornblende gabbro from East Kunlun Orogenic Belt and its constraints on evolution of Paleo- Tethys occean[J]. Earth Science, 43(2): 354-370(in Chinese with English abstract).

附中文参考文献

奥琮,孙丰月,李碧乐,王冠,李良,李世金,赵俊伟. 2015. 东昆仑祁漫塔格地区小尖山辉长岩地球化学特征、U-Pb年代学及其构造意义[J]. 大地构造与成矿学, 39(6): 1176-1184.

陈邦学, 徐胜利, 杨有生, 周能武, 朱志新. 2019. 东昆仑西段其木来克一带晚二叠世侵入岩的成因及其构造意义. 地质通报, 38(6): 1040-1051.

陈国超. 2014. 东昆仑造山带(东段)晚古生代—早中生代花岗质岩石特征、成因及地质意义[D]. 西安: 长安大学, 1-181.

陈守建, 李荣社, 计文化, 赵振明, 刘荣丽, 贾宝华, 张振福, 王国灿. 2010. 昆仑造山带二叠纪岩相古地理特征及盆山转换探讨[J]. 中国地质, 37(2): 374-393.

陈有炘, 裴先治, 李瑞保, 刘战庆, 李佐臣, 张晓飞, 陈国超, 刘智刚, 丁仨平, 郭俊锋. 2011. 东昆仑造山带东段元古界小庙岩组的锆石U-Pb年龄[J]. 现代地质, 25(3): 510-521.

甘彩虹. 2014. 青海东昆仑造山带火成岩岩石学、地球化学、锆石U-Pb年代学及Hf同位素特征研究[D]. 北京: 中国地质大学(北京), 1-75.

郭正府, 邓晋福, 许志琴, 莫宣学, 罗照华. 1998. 青藏东昆仑晚古生代末—中生代中酸性火成岩与陆内造山过程[J]. 现代地质, 12(3): 344-352.

菅坤坤, 魏燕霞, 施彬, 刘力, 王星, 袁璋. 2015. 东昆仑造山带中灶火地区早中生代镁铁质岩墙群的成因及地质意义[J]. 中国地质, 42(5): 1457-1470.

姜春发, 王宗起, 李锦轶. 2000. 中央造山带开合构造[M]. 北京: 地质出版社, 1-154.

姜春发, 杨经绥, 冯秉贵, 朱志直, 赵民, 柴耀武, 施希德, 王怀达, 胡金庆. 1992. 昆仑开合构造[M]. 北京: 地质出版社, 183-217.

孔会磊, 李金超, 栗亚芝, 贾群子, 国显正. 2017a. 青海东昆仑东段加当辉长岩LA-ICP-MS锆石U-Pb测年及其地质意义[J]. 地质与勘探, 53(5): 889-902.

孔会磊, 李金超, 栗亚芝, 贾群子, 国显正, 王宇. 2017b. 青海东昆仑哈陇休玛辉石橄榄岩LA-ICP-MS锆石U-Pb测年及其地质意义[J]. 地质科技情报, 36(1): 41-47.

孔会磊, 李金超, 栗亚芝, 贾群子, 国显正, 张斌. 2018. 青海东昆仑东段加当橄榄辉长岩锆石U-Pb年代学、地球化学及地质意义[J]. 地质学报, 92(5): 964-978.

孔会磊, 栗亚芝, 李金超, 贾群子, 国显正, 张斌. 2019. 东昆仑希望沟橄榄辉石岩LA-ICP-MS锆石U-Pb定年及岩石地球化学特征[J]. 地质力学学报, 25(3): 440-452.

李荣社, 计文化, 杨永成, 于浦生, 赵振明, 陈守建, 孟勇, 潘晓平, 史秉德, 张维吉, 李行, 洛长义. 2008. 昆仑山及邻区地质[M]. 北京: 地质出版社, 1-400.

李瑞保, 裴先治, 李佐臣, 刘战庆, 陈国超, 陈有炘, 魏方辉, 高景民, 刘成军, 裴磊. 2012. 东昆仑东段晚古生代—中生代若干不整合面特征及其对重大构造事件的响应[J]. 地学前缘, 19(5): 244-254.

李瑞保. 2012. 东昆仑造山带(东段)晚古生代—早中生代造山作用研究[D]. 西安: 长安大学, 1-173.

陆松年. 2002. 青藏高原北部前寒武纪地质初探[M]. 北京: 地质出版社, 1-125.

罗明非, 莫宣学, 喻学惠, 李小伟, 黄雄飞. 2015. 东昆仑五龙沟晚二叠世花岗闪长岩LA-ICP-MS锆石U-Pb定年、岩石成因及意义[J]. 地学前缘, 22(5): 182-195.

罗照华, 邓晋福, 曹永清, 郭正府, 莫宣学. 1999. 青海省东昆仑地区晚古生代—早中生代火山活动与区域构造演化[J]. 现代地质, 13(1): 51-56.

莫宣学, 罗照华, 邓晋福, 喻学惠, 刘成东, 谌宏伟, 袁万明, 刘云华. 2007. 东昆仑造山带花岗岩及地壳生长[J]. 高校地质学报, 13(3): 403-414.

王亚磊, 张照伟, 张江伟, 钱兵, 刘月高, 尤敏鑫. 2017. 东昆仑造山带早中生代幔源岩浆事件及其地质意义[J]. 地质与勘探, 53(5): 855-866.

吴福元, 李献华, 郑永飞, 高山. 2007. Lu-Hf同位素体系及其岩石学应用[J]. 岩石学报, 23(2): 185-220.

熊富浩, 马昌前, 张金阳, 刘彬. 2011a. 东昆仑造山带早中生代镁铁质岩墙群LA-ICP-MS锆石U-Pb定年、元素和Sr-Nd-Hf同位素地球化学[J]. 岩石学报, 27(11): 3350-3364.

熊富浩, 马昌前, 张金阳, 刘彬, 蒋红安, 黄坚. 2011b. 东昆仑造山带白日其利辉长岩体LA-ICP-MS锆石U-Pb年龄及地质意义[J]. 地质通报, 30(8): 1196-1202.

熊富浩. 2014. 东昆仑造山带东段古特提斯域花岗岩类时空分布、岩石成因及其地质意义[D]. 武汉: 中国地质大学, 1-174.

许志琴, 杨经绥, 李海兵, 张建新, 吴才来. 2007. 造山的高原—青藏高原的地体拼合、碰撞造山及隆升机制[M]. 北京: 地质出版社, 1-458.

杨经绥, 许志琴, 李海兵, 史仁灯. 2005. 东昆仑阿尼玛卿地区古特提斯火山作用和板块构造体系[J]. 岩石矿物学杂志, 24(5): 369-380.

杨延乾, 李碧乐, 许庆林, 张炳社. 2013. 东昆仑埃坑德勒斯特二长花岗岩锆石U-Pb定年及地质意义[J]. 西北地质, 46(1): 56-62.

殷鸿福, 张克信. 1997. 东昆仑造山带的一些特点[J]. 地球科学: 中国地质大学学报, 22(4): 339-342.

张玉, 裴先治, 李瑞保, 刘成军, 陈有炘, 李佐臣, 王兴, 胡晨光, 颜全治, 彭思钟. 2017. 东昆仑东段阿拉思木辉长岩锆石U-Pb年代学、地球化学特征及洋盆闭合时限界定[J]. 中国地质, 44(3): 526-540.

赵旭, 付乐兵, 魏俊浩, 赵玉京, 唐洋, 杨宝荣, 管波, 王晓云. 2018. 东昆仑按纳格角闪辉长岩体地球化学特征及其对古特提斯洋演化的制约[J]. 地球科学, 43(2): 354-370.